Volume 1 | Number 1 | Jan 2013 | Pages 1–100

Dalton Transactions

An international journal of inorganic chemistry
www.rsc.org/dalton

ROYAL SOCIETY OF CHEMISTRY

This is an *Accepted Manuscript*, which has been through the Royal Society of Chemistry peer review process and has been accepted for publication.

Accepted Manuscripts are published online shortly after acceptance, before technical editing, formatting and proof reading. Using this free service, authors can make their results available to the community, in citable form, before we publish the edited article. We will replace this *Accepted Manuscript* with the edited and formatted *Advance Article* as soon as it is available.

You can find more information about *Accepted Manuscripts* in the **Information for Authors**.

Please note that technical editing may introduce minor changes to the text and/or graphics, which may alter content. The journal's standard **Terms & Conditions** and the **Ethical guidelines** still apply. In no event shall the Royal Society of Chemistry be held responsible for any errors or omissions in this *Accepted Manuscript* or any consequences arising from the use of any information it contains.

www.rsc.org/dalton

The mechanism of the Cu^{2+}[12-MC$_{Cu(Alaha)}$-4] metallacrown formation and Lanthanum(III) encapsulation

Maria R. Beccia[a], Begoña García[b], Javier García-Tojal[b], José M. Leal[b], Fernando Secco*[c],*

Matteo Tegoni[d]

[a]CEA, DSV, IBEB, Laboratoire des Interactions Protéine Métal, CNRS UMR Biologie Végétale et Microbiologie Environnementale, Université d'Aix-Marseille, Saint-Paul-lez-Durance, France

[b]Department of Chemistry, University of Burgos, Plaza Misael Bañuelos s/n., 09001 Burgos, Spain

[c]Department of Chemistry and Industrial Chemistry, University of Pisa, Via Risorgimento 35, 56126 Pisa, Italy.

Fax +390502219260, e-mail ferdi@dcci.unipi.it

[d]Department of Chemistry, University of Parma, Viale G.P. Usberti, 17A, 43100, Parma, Italy

Abstract A kinetic, calorimetric and EPR study has been performed on the formation of the metallacrown Cu^{2+}[12-MC$_{Cu(Alaha)}$-4] from Cu(II) and α-alaninehydroxamic acid (H$_2$L). The acidity range where Cu^{2+}[12-MC$_{Cu(Alaha)}$-4] is stable lies between pH 3.5 and 6.0. For pH values below that range the complex CuHL$^+$ is the prevailing species. This species plays a fundamental role in the formation of Cu^{2+}[12-MCCu(Alaha)-4]. Actually, depending on the Cu(II)/H$_2$L ratio and on pH, it can originate a dimer $Cu_2(HL)_2^{2+}$ or a dinuclear complex Cu_2L^{2+}. Both species constitute the nuclei necessary for a further oligomerisation reaction which ends when the crown is formed. The kinetics of Cu^{2+}[12-MC$_{Cu(Alaha)}$-4] formation is biphasic. Under conditions of Cu(II) excess the fast phase leads to formation of Cu_2L^{2+}. The slow phase is interpreted in terms of a sequential addition of monomers (CuHL$^+$) to the Cu_2L^{2+} nucleus to form the crown.

The interaction of La(III) with Cu^{2+}[12-MC$_{Cu(Alaha)}$-4] has also been investigated. The system displays a biphasic behaviour; in the first phase the intermediate complex Cu[12-MC$_{Cu(Alaha)}$-4]La is formed which, in excess of ligand, evolves towards the larger metallacrown La^{3+}[15-MC$_{Cu(Alaha)}$-5]. The reaction mechanisms of the two investigated systems are discussed.

1

Introduction

Metallacrowns (MCs) are an interesting class of self-assembled metallamacrocycles, which form in solution when the proper conditions (metal-to-ligand stoichiometric ratio and pH) are satisfied.[1-3] They contain a metal-ligand coordination framework, which constitutes the metallacrown architecture and they are characterized by the presence of a core cavity, which may encapsulate a variety of cations and anions. This property provides the basis for the potential use of MCs as recognition agents.[2] MCs can be considered the inorganic analogues of crown ethers, as their scaffold is conceptually obtained by replacing the methylene carbons of crown ethers with metal-heteroatom coordination units, -[M-N-O]-. As in crown ethers, MCs are defined on the basis of the ring size and the number of donating oxygen atoms. In the present study $Cu^{2+}[12\text{-}MC_{Cu(Alaha)}\text{-}4]$ denotes a 12-membered ring comprising 4 repeating -[M-N-O]- sequences where M=Cu whereas the nitrogen and oxygen atoms are provided by alaninehydroxamic acid (Alaha) (Figure 1). In addition to the ring metal ions involved in the bridging coordination of the ligands, MCs are able to selectively encapsulate a further core metal ion (in this study Cu^{2+} or La^{3+}) in the central oxygen cavity.[1,4,5] Since their discovery in 1989 by Pecoraro and Lah,[6,7] the chemistry of MCs has largely expanded. In particular, MCs obtained with aminohydroxamic acids and copper(II) as the ring metal ion have been the most studied and, probably, the most interesting owing to the large variability of structures obtained in the solid state[4] and because of their solubility in water.[3] To date, a number of copper(II) /aminohydroxamic acids MCs have been isolated and extensively characterized in the solid state.[3] The enlightenment of the mechanism of metallacrown self-assembly process in solution is a key point if one conceives solution-based applications of metallacrowns, for example, as sequestering agents for selective cation and anion recognition.[8-11] However, despite the number of investigations performed to assess the structural properties and stability of copper(II)

2

/aminohydroxamic acids MCs in solution,[3,12-18] no specific studies on the mechanism of their self-assemblies with the possible identification of transient species are reported so far in the literature.

 In this paper we present a kinetic and thermodynamic study of the copper(II)-α-aminohydroximate system in aqueous solution to give the $Cu^{2+}[12-MC_{Cu(Alaha)}-4]$ MC shown in Figure 1 and of the process of encapsulation of La^{3+} in the cavity of $Cu^{2+}[12-MC_{Cu(Alaha)}-4]$ to give the species $La^{3+}[15-MC_{Cu(Alaha)}-5]$

Experimental

Chemicals (S)-α-Alaninehydroxamic acid (Alaha) was synthesized as reported in the literature and its purity checked by NMR and elemental analysis.[16] Aqueous stock solutions of the ligand were prepared by weighing appropriate amounts of the solid reagent (purity = 99%). These solutions were used within 3–4 days. All the other chemicals were analytical grade reagents from Sigma Aldrich. A stock solution of copper chloride was prepared dissolving the appropriate amount of $CuCl_2 \cdot H_2O$ in pure water and the Cu(II) concentration was measured by titration with EDTA. Lanthanum chloride heptahydrate (>99.9% pure) was dissolved in water. Hydrochloric acid and potassium chloride of known concentration were used to attain the desired medium acidity and ionic strength, respectively. Acetic buffer solution (pH = 4.5, 0.1 M) was prepared by weighing the appropriate amount of sodium acetate ($CH_3COONa \cdot 3H_2O$, 99.5% Sigma) and dissolving it in acetic acid (CH_3COOH, 99.5% Sigma). All solutions were prepared with doubly distilled water.

Methods The hydrogen ion concentrations of the working solutions were determined using a Metrohm 713 pH-meter equipped with a combined glass electrode, which was calibrated by means of HCl solutions of known concentrations.[19] This procedure enables the pH-meter to yield directly the values of $-\log[H^+]$.

Differential scanning calorimetry measurements have been performed with a TA Instruments nano DSC apparatus. Thermochemical measurements were carried out using solutions carefully stirred and degassed under vacuum for 15 minutes prior to use. A 0.30 mL sample containing both metal

([CuCl$_2$] = 1×10^{-2} M) and ligand in the ratio 5:4, at pH = 4.5 and I = 0.1 M (KCl) was placed in the sample capillary cell. The reference solution, prepared at the same pH and I values without Alaha and CuCl$_2$, was placed in the reference capillary cell. The measurements were started at a scan rate 1°C/min and P = 1.5 atm. The pH was varied in the range 3 to 8, in order to observe the thermal behavior of the different species formed at different pH values[20]. Isothermal calorimetric titrations were performed at 25°C using a TA Instruments nano ITC device. In a typical titration, 1 μL of a 0.17 M aqueous solution of Alaha was injected at equal intervals of 300 s to the CuCl$_2$ solution (0.033 M), already present in the sample cell, while stirring at 300 rpm. In total 50 μL of Alaha solution were added to the CuCl$_2$ solution. The reference cell of the calorimeter was filled with ultrapure water and both cells were maintained at the same temperature. After addition of Alaha solution to CuCl$_2$ solution, the heat flux needed to keep both the sample cell and reference cell at the same temperature was monitored. The heat released by the dilution of CuCl$_2$ was neglected, being very small.[21] All calorimetric analyses were evaluated with the fitting package Nano Analyze. Fast Atom Bombardment (FAB)-Mass spectrometry measurements were recorded on a VG AutoSpec apparatus, using an ionization liquid secondary ion mass spectrometer (LSMIS$^+$), Cs$^+$ as bombarding ions and thioglycerol as the matrix. Solutions containing CuCl$_2$ and Alaha (M:L = 5:4, C$_M$ = 1.25×10^{-2} M) were prepared at different pH values, ranging between 2 and 10, and I = 0.1 M (KCl). Electrospray-assisted mass spectrometric analyses (ESI-MS) were performed on a MicroTOF-Q (Bruker) with an electrospray ionization source. Aqueous solutions to be analyzed were diluted 1:10 in CH$_3$OH. The samples were continuously infused at a 3 μL/min flow rate. Mass spectra were recorded in the 50–6000 mass-to-charge (*m/z*) range. MS experiments were carried out with a capillary voltage set at 4.5 kV and an end plate off-set voltage of 500 V. The gas nebulizer (N$_2$) pressure was set at 0.4 bar and the dry gas flow (N$_2$) at 4 L/min at 190°C. Data were acquired in the positive mode and calibration was performed using a calibrating solution of ESI Tune Mix (Agilent) in CH$_3$CN/H$_2$O (95/5 v/v). The system was controlled by the software package MicroTOF Control 2.2 and data were processed with DataAnalysis 3.4. For the analysis of the decomposition

of the 12-MC-4 complex the solution has been prepared as follows: A solution containing Cu^{2+} and ligand (Cu:L=5:4, $[CuCl_2]=1\times10^{-3}$ M) was prepared at pH = 4.5 (acetate buffer). ESI-MS analysis of this solution was performed before and after heating (90 °C, 3 hours). For the analysis of the formation of the 15-MC-5 complex the solution has been prepared as follows: a solution containing Cu^{2+}, and the ligand was added with La^{3+} to obtain a final La:Cu:L=1:5:5 molar ratio ($[CuCl_2]=1\times10^{-3}$ M) was prepared at pH = 4.5 (acetate buffer).

The EPR experiments were performed on a Bruker EMX spectrometer, equipped with a Bruker ER 036TM NMR-teslameter and an Agilent 53150A microwave frequency counter to fit the magnetic field and the frequency inside the cavity. The simulation of the EPR spectra was performed using the SimFonia program provided by Bruker, whereas different fits were combined with the Kaleidagraph v3.5 program to achieve final spectra and graphics. Tipically, 500 μl of the Alaha solution were added to 500 μl of the $CuCl_2$ solution (both solutions being brought at pH 4.5 with acetic acid/acetate 0.015 M buffer and ionic strength 0.1 M KCl). Afterwards, 200 μl of the mixture were poured into the tube of the flat cell. Solutions in quartz tubes, frozen in a nitrogen-containing Dewar to avoid any precipitation, were put into the continuous flow cryostat in the resonance cavity. In the reactions with La(III) ions, 100 µl of the La(III) solution were added to 100 µl of the above described Cu(II) + HL solution.

The UV-vis measurements were performed on a Perkin-Elmer Lambda 35 double beam spectrophotometer. The apparatus is equipped with jacketed cell holders, with a temperature control to within ±0.1°C. Titrations of Alaha with Cu(II) were carried out at a fixed wavelength, by addition of increasing amounts of metal to the spectrophotometric cell containing the ligand solution. The thermal stability of $Cu^{2+}[12\text{-}MC_{Cu(Alaha)}\text{-}4]$ was investigated between 20 °C and 90 °C, with a scan rate of 1°C/min and an equilibration time of 2 min after each temperature increase.

The kinetic experiments were carried out using a stopped-flow apparatus, assembled in our laboratory: the apparatus uses a HI-TECH KinetAsyst SF-61SX2 mixing unit, connected to a spectrophotometric line by two optical guides; the radiation, produced by a Hamamatsu L248102

Xenon 'quiet' lamp, is passed through a Baush and Lomb 338875 high intensity monochromator and then split into two beams. The reference beam is directly sent to a 1P28 photomultiplier, while the second beam passes through the sample and is then collected by a second 1IP28 photomultiplier. The outputs of the two beams are equilibrated before each shot. The kinetic curves were stored on a Tektronix digital oscilloscope and at least 5 repeated experiments were done for each sample. The kinetic curves were analyzed by a non-linear least-square fitting procedure performed by the Jandel statistical package which makes use of the Marquardt algorithm.[22] The observed spread of the kinetic parameters was confined to within 10%.

Results

Formation and decomposition of $Cu^{2+}[12-MC_{Cu(Alaha)}-4]$

The fully protonated α-alaninehydroxamic acid is here denoted as H_3L^+ since all the three acid protons are involved in the metallacrown formation. The copper/Alaha complexes are formulated by consequence. For the sake of simplicity, the species $Cu^{2+}[12-MC_{Cu(Alaha)}-4]$ will be denoted as $Cu^{2+}[12-MC-4]$.

Thermal stability experiments. The thermal stability of the Cu(II)/Alaha metallacrown has been investigated by means of differential scanning calorimetry (DSC) and UV-Vis experiments.

DSC Analysis. A DSC experiment regarding the thermal decomposition of $Cu^{2+}[12-MC-4]$ is shown in Figure 2. The important exothermic peak appearing at 90°C has been ascribed to the disassembly of the metallacrown according to reaction (1)

$$Cu_5L_4^{2+} + 12H^+ \rightleftarrows 5Cu^{2+} + 4H_3L^+ \tag{1}$$

where $Cu_5L_4^{2+}$ represents $Cu^{2+}[12-MC-4]$. The large negative enthalpy value obtained for reaction (1) (-160 kJ.mol^{-1} estimated from the area of the related thermal curve) indicates that reaction (1) is the result of the combination of two processes, one of them being endothermic (ring rupture) and the other largely exothermic.

UV-Vis Analysis. Figure 3A shows the spectral behavior of the Cu^{2+}/Alaha system recorded at pH = 4.5. The presence of a large amount of the metallacrown is revealed by an intense band with maximum absorption at 340 nm (spectrum (a)). Under the same conditions the free reactants exhibit a much weak absorption (spectra (b) and (c)). Figure 3B shows the thermal decomposition of the metallacrown. The plot represents the decrease of absorbance at 340 nm of a solution containing the assembled Cu^{2+}[12-MC-4] recorded on rising the temperature from 20 to 90°C. The signal remains almost constant up to T = 73 °C and then displays an abrupt decrease. Comparison with Figure 3A provides evidence for the endothermic disassembly of the metallacrown[9] (see discussion) at a relatively high temperature.

The range of pH where the metallacrown is stable is rather limited. At pH = 3 no change of absorbance could be detected on adding Cu^{2+} ions to a solution of Alaha (Figure 1S), however, according to the literature,[9,18] strong interactions between metal and ligand become effective slightly above that pH value. The 1:1 complex, $CuHL^+$ has been supposed to form first, on the basis of pHmetric titrations.[13,23,24] Then, formation of the Cu^{2+}[12-MC-4] metallacrown does occur, reaching its maximum extent at pH=4.5.[13] However, the presence of noticeable amounts of a dimer $Cu_2L_2H^+$ at this pH value has been inferred from titration analysis.[23] The proposed structure of the dimer (reported in Scheme 1 as D2) involves Cu^{2+} coordination also to the hydroxamate oxygen atoms. Thus, it is conceivable that, under conditions of large metal excess, a dinuclear complex of the type Cu_2L^{2+} could be formed, where the NN and the OO sites of a single Alaha molecule bind two Cu^{2+} ions (structure D3 in scheme 1).

Isothermal titration calorimetry An isothermal calorimetric titration has been performed at pH = 4.5 and $I = 0.1$ M, by adding increasing amounts of Alaha to a solution of $CuCl_2$. The titration curve shows two equivalent points at copper-to-ligand ratios of 2:1 and 5:4 respectively (Figure 4). This result provides evidence for metallacrown formation, but also reveals the presence of a dinuclear complex, Cu_2L, under conditions of metal excess.

FAB-mass spectrometry. The mass spectrometry experiments on the Cu(II)/Alaha system have

been performed in the pH range between 2 and 10. The resulting FAB-MS spectra (Figure 2S) contain a mass envelope corresponding to $[Cu_5L_4]Cl^+$ (M/Z = 761); this finding further attests to the stability of the $Cu^{2+}[12$-MC-4] species in aqueous solution. Under high voltage conditions, fragmentation of the pentanuclear species was obtained, consistently with previous ESI-MS data.[20] Noticeable amounts of the tetramer $[Cu_4L_4]H^+$ (M/Z = 664) were also detected.

ESI-mass spectrometry. The 12-MC-4 decomposition and La(III)-15-MC-5 formation were investigated by ESI-mass spectrometry. The ESI-MS analysis of the solution containing Cu^{2+} and the ligand in 5:4 molar ratio was performed before and after heating for 3 hours at 90°C . The ESI-MS spectra collected before heating contain the mass envelope corresponding to $[Cu_5L_4]Cl^+$ (*m/z*=761) as shown in Figure 3S. The absence of this peak in spectra recorded after heating at 90 °C (Figure 4S) confirms the decomposition of 12-MC-4 under these conditions.

Kinetics.

 The kinetics of the reaction have been investigated by the stopped-flow technique at λ = 340 nm and I = 0.1 M (KCl). The experiments performed under conditions of metal excess, reveal a biphasic behaviour (Figure 5).

The fast phase. The orders of reaction with respect to Cu^{2+} and Alaha were determined for the fast phase of the reaction from the slopes of logv° vs. log C_i plots,[25,26] where v° is the initial reaction rate and C_i are, in turn, the concentrations of metal and ligand (Figure 5S and 6S). The reaction orders were found to be equal to 1.3 with respect to Cu^{2+} and 1.4 with respect to Alaha. The fractional values, higher than one, indicate that the fast phase of the reaction is composed by (at least) two steps, one of them being second-order with respect to metal and ligand, the other being first-order. Experiments performed at different concentrations of the reactants under the condition $C_{Cu} = C_L$ allowed to determine the global reaction order of the fast phase that turned to be 2.7 (Figure 7S), in good agreement with the sum of the individual reaction orders.

The effect of the ionic strength on the reaction rates of the fast phase has been studied by stopped-

flow experiments keeping constant the reactant concentrations and the pH value (pH = 4.5) and varying the level of added salt (KCl, Figure 6). The use of sodium perchlorate provided results similar to those obtained with KCl. The dependence of the initial rate on the ionic strength has been found to be linear according to the Güntelberg equation (equation (2)).[27,28]
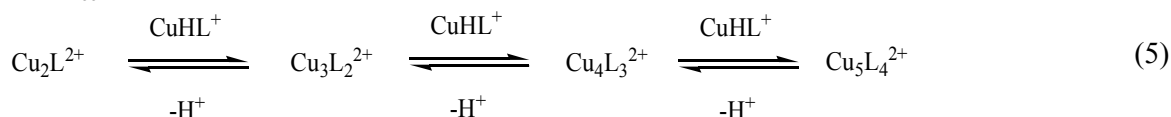
$$\log v° = \log v°_{I=0} + 1.01 Z_A Z_B \frac{I^{1/2}}{1 + I^{1/2}} \tag{2}$$

where the parameter $v°_{I=0}$ is the initial rate at $I = 0$ and $Z_A Z_B$ is an apparent product of the charges of the reactants. The fractional value of $Z_A Z_B$ obtained from the slope of the straight line of Figure 6 (0.8 ± 0.1) reveals the presence of an ionic strength dependent pre-equilibrium. This result and the fractional reaction orders can be rationalized by reactions (3) and (4) of the reaction scheme (3)-(5).

Fast effect

$$Cu^{2+} + H_3L^+ \underset{}{\overset{K_1}{\rightleftharpoons}} CuHL^+ + 2H^+ \tag{3}$$

$$2\,CuHL^+ \underset{k_{-2}}{\overset{k_2}{\rightleftharpoons}} Cu_2L^{2+} + H_2L \tag{4}$$

Slow effect

$$Cu_2L^{2+} \overset{CuHL^+}{\underset{-H^+}{\rightleftharpoons}} Cu_3L_2^{2+} \overset{CuHL^+}{\underset{-H^+}{\rightleftharpoons}} Cu_4L_3^{2+} \overset{CuHL^+}{\underset{-H^+}{\rightleftharpoons}} Cu_5L_4^{2+} \tag{5}$$

Step (3) is too fast to be directly observed using the stopped-flow method, but its presence is suggested by the non-integer reaction orders and by the fact that the $Z_A Z_B$ value is lower than expected. The initial rate of the fast phase, $v°$, is expressed by equation (6), which has been derived as described in the Supporting Information.

$$v^\circ = \frac{k_2 C_L C_{Cu}}{\{1 + [H^+]^2 / K_1 C_{Cu}\}\{1 + [H^+]^2 / K_1 C_L\}}$$ (6)

In equation (6) K_1 is the equilibrium constant of step (3), whereas k_2 is the forward rate constant of step (4). Equation (6) justifies the fact that the reaction order with respect to metal and ligand lies between 1 and 2. Actually, for $[H^+]^2/K_1C_{Cu} \ll 1$ and $[H^+]^2/K_1C_L \ll 1$ the order of reaction with respect to each reactant tends to unity. Oppositely, for $[[H^+]^2/K_1C_{Cu} \gg 1$ and $[H^+]^2/K_1C_L \gg 1$, the reaction order tends to 2.

The situation changes if a considerable excess of metal is used. Actually, for $C_{Cu} \geq 10C_L$, the fast phase displays monoexponential kinetic curves (Figure 8S) from which the time constant, $1/\tau_f$, is evaluated. The dependence of $1/\tau_f$ on C_{Cu} is linear (Figure 7) and this result indicates that, in excess of Cu^{2+}, reaction (4) is replaced by reaction (7).

$$Cu^{2+} + CuHL^+ \rightleftarrows Cu_2L^{2+} + H^+$$ (7)

Under these circumstances the kinetic behavior of the fast effect is represented by equation (8) (Supporting Information)

$$\frac{1}{\tau_f} = \frac{K'_1 k_2 C_{Cu}^2}{1 + K'_1 C_{Cu}} + k'_{-2}$$ (8)

where $K'_1 = K_1/[H^+]^2$ and $K'_1C_{Cu} \gg 1$ (actually, according to the data of ref [13,20], $K_1 = 41$, thus, being these experiments performed at pH = 4.5, $K'_1 = 2.6\times10^{10}$ M^{-1}). Data analysis yields $k_2 = 0.18 \pm 0.01$ s^{-1}M^{-1} and $k_{-2}' = 19 \pm 3$ s^{-1}. The absence of rate dependence on $[H_3L^+]$ of the kinetics of complex dissociation (not shown) reveals that this species is not involved in the reverse process.

The slow phase. The slow phase (Figure 5) is observed only for Cu(II)/Alaha concentration ratios

10

close to M:L = 5:4. The amplitude of the slow kinetic effect has been measured at 340 nm between

pH 2.5 and 7.0, keeping constant the ionic strength and the metal and ligand concentrations (with

$C_M : C_L = 5:4$, according to the Cu^{2+}[12-MC-4] stoichiometry). The plot of the amplitude vs. pH

displays a bell-shaped trend (Figure 8), with a maximum value at about pH = 5. This plot is

analogous to the curve that, in the speciation diagram of the Cu(II)/Alaha system, corresponds to

the Cu^{2+}[12-MC-4] metallacrown.[20] In contrast, at pH values lower than 3.4 and higher than 7,

where Cu^{2+}[12-MC-4] does not exist, no measurable amplitude could be detected. Actually, at pH

values less than 3.4, the extent of binding is negligible, whereas for pH values higher than 7 the 1:2

complexes are the dominant species.[15] The analysis of the direct (formation) process of the slow

phase becomes more complex, as the pseudo-first order conditions cannot be accomplished.

Therefore, the reverse reaction, corresponding to the decomposition of the pre-assembled Cu^{2+}[12-

MC-4] induced by the addition of HCl, has been investigated. For this purpose, a series of

experiments has been devised where known amounts of HCl in excess have been added to solutions

containing Cu^{2+}[12-MC-4]. A kinetic curve of the disassembly process is displayed in Figure 9S.

The dependencies of the amplitude (A_{diss}) and the rate constant ($1/\tau_{diss}$) of the MC decomposition

reaction on [H^+] are shown in Figures 9A and 9B respectively. The increase of the amplitude values

with the acid level reveals that reaction (5) is an equilibrium process, whose position is controlled

by the protons concentration. Reversibility of step (5) is confirmed by the plot of Figure 9B, where

the positive value of the intercept reveals that also the MC formation step is present. The first order

dependence of $1/\tau_{diss}$ on acid concentration denotes the involvement of just one proton in the rate-

determining step of the Cu^{2+}[12-MC-4] disassembly.

The interaction of La(III) with Cu^{2+}[12-MC$_{Cu(Alaha)}$-4]

Equilibria. The interaction of La(III) with Cu^{2+}[12-MC-4] to give the bigger La^{3+}[15-MC$_{Cu(Alaha)}$-5]

metallacrown (denoted as La[15MC-5] from now on), where a La(III) ion is encapsulated in the

centre of the ring, is revealed by spectral changes in the visible region. In order to see if the

interaction is reversible, spectrophotometric titrations of the preformed Cu^{2+}[12-MC-4] with $LaCl_3$. A typical binding curve is shown in Figure 10A. The titrations were analyzed according to equation (9) which holds for the employed experimental conditions ($C_{La} >> C_{12MC4}, C_L$).
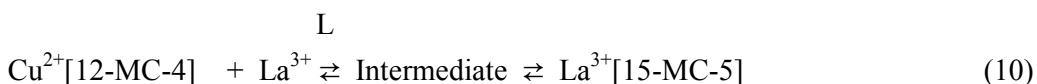
$$\frac{\Delta A / \Delta \varepsilon}{(C_{12MC4} - \Delta A / \Delta \varepsilon) \times (C_L - \Delta A / \Delta \varepsilon)} = K \times C_{La} \qquad (9)$$

$\Delta A / \Delta \varepsilon$ corresponds to the equilibrium concentration of La[15-MC-5], $\Delta A = A - A_0$ being A_0 the initial absorbance, $\Delta \varepsilon = \varepsilon_{product} - \varepsilon_{reactant}$.

The slope of the straight line obtained according to equation (9) provides the equilibrium constant, K (Figure 10B).

Kinetics. The kinetics of Cu^{2+}[12-MC-4] interaction with La(III) have been investigated under pseudo first-order conditions ($C_{La} >> 10C_{Cu[12-MC-4]}$). The spectrophotometric cell contained a solution of the preformed Cu^{2+}[12-MC-4] and an equimolar amount of the ligand (L) at the desired pH, ionic strength and temperature. A calibrated excess of $LaCl_3$ solution was added to the mixture in the cell and the time course of the reaction was recorded.

Rate dependence on La(III) concentration. The reacting system displays a biphasic behaviour (Figure 11A) that can be represented by the sequence (10).

$$Cu^{2+}[12\text{-}MC\text{-}4] \ + \ La^{3+} \ \overset{L}{\rightleftarrows} \ Intermediate \ \rightleftarrows \ La^{3+}[15\text{-}MC\text{-}5] \qquad (10)$$

The analysis of the kinetic traces provides the amplitudes and time constants, $1/\tau_{fast}$ and $1/\tau_{slow}$, of the two phases. Experiments carried out varying the La(III) concentration reveal the behaviors shown in Figure 12. The positive intercepts of the two plots shown in Figure 12 indicate that reaction (10) is an equilibrium processes. Concerning the fast phase, the linear dependence of $1/\tau_{fast}$ on C_{La} (Figure 12 A) is interpreted according to equation (11) [29,30] which yields the values of the

$$\frac{1}{\tau_{fast}} = k_{f,fast}C_{La} + k_{d,fast} \tag{11}$$

apparent rate constants for the forward ($k_{f,fast}$) and reverse ($k_{d,fast}$) step. Concerning the slow effect, the dependence of $1/\tau_{slow}$ on the La(III) concentration (Figure 12B) agrees with equation (12).[31,32]

$$\frac{1}{\tau_{slow}} = \frac{K_{app,fast}k_{f,slow}C_{La}}{1 + K_{app,fast}C_{La}} + k_{d,slow} \tag{12}$$

According to sequence (10), the overall apparent equilibrium constant, K_{app}, should be a function of the rate constants of the two phases, as shown in equation (13).

$$K_{app} = \frac{k_{f,fast}}{k_{d,fast}}\left(1 + \frac{k_{f,slow}}{k_{d,slow}}\right) \tag{13}$$

The value of K_{app} obtained from kinetics is in good accordance with that resulting from the spectrophotometric analysis, thus confirming that the scheme (10) describes appropriately the apparent reaction sequence. The values of the reaction parameters are collected in Table 1.

Rate dependence on Cu(II) concentration. In order to investigate the role of copper(II) in the reaction mechanism, three series of experiments have been performed where the rate dependence on the La(III) concentration has been measured. In each series a constant excess of Cu(II) was present and the three series differed for the copper content. No excess ligand was present in this case, thus 15-MC-5 could not form. Under these circumstances the kinetic curves are mono-exponential (Figure 11B) and data analysis shows that they correspond to the fastest of the two phases.

The results are shown in Figure 13. The slope and the intercept of each straight line correspond to $k_{f,fast}$ and $k_{d,fast}$, respectively according to equation (11). While $k_{f,fast}$ is independent of the copper(II)
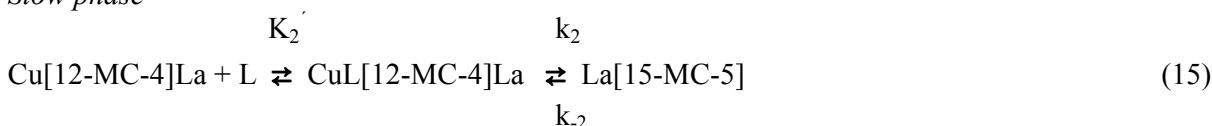
concentrations, $k_{d,fast}$ increases when raising the Cu(II) content. This result provides evidence for the involvement of Cu(II) in the reverse step of the fast process. In the light of this finding, it is reasonable to suppose that, in the fast step, the copper ion allocated in the core of Cu^{2+}[12-MC-4] is released.

Rate dependence on Alaha concentration. The rate dependence on Alaha concentration (C_L) has been investigated under the conditions $C_L > C_{La} > C_{12MC4}$. In excess of ligand the system displays a biexponential behaviour. The time constant of the fast process, $1/\tau_{fast}$, was found to be independent of the ligand concentration (Figure 14A), while the slowest time constant, $1/\tau_{slow}$, increases tending to a plateau, as shown in Figure 14B. The behaviour shown in Figure 14 reveals that the ligand is not involved in the fast phase of the process while it plays a role in the slow phase. In the light of the kinetic results the apparent sequence (10) can be rationalized on the basis of the detailed reaction scheme (14)-(15) (charges omitted).

Fast phase:

$$\text{Cu[12-MC-4] + La} \underset{k_{-1}}{\overset{K_1'\qquad\qquad k_1}{\rightleftarrows\quad\text{Cu[12-MC-4]La}\ \rightleftarrows}} \text{La[12-MC-4] + Cu} \qquad (14)$$

Slow phase

$$\text{Cu[12-MC-4]La + L} \underset{k_{-2}}{\overset{K_2'\qquad\qquad k_2}{\rightleftarrows\quad\text{CuL[12-MC-4]La}\ \rightleftarrows}} \text{La[15-MC-5]} \qquad (15)$$
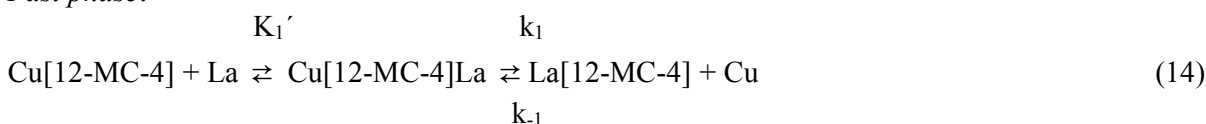
The time constant of the fast phase is expressed by equation (16) (see supporting Information)

$$\frac{1}{\tau_{fast}} = \frac{K_1' k_1 C_{La}}{1 + K_1' C_{La}} + k_{-1} C_{Cu} \qquad (16)$$

The first step of the sequence (14) equilibrates very fast to give the intermediate species Cu[12-MC-4]La which evolves towards the La[12-MC-4] complex in the second (rate determining) step of the

fast phase. This step involves the expulsion of a copper ion, as indicated by the increase of $k_{d,fast}$ on raising the level of Cu^{2+} ions in the reacting solution (Figure 13). If K_1', the formation constant of the complex Cu[12-MC-4]La, is small as expected, then it turns out that in equation 16 $K_1'C_{La}$ << 1 and the linear dependence of $1/\tau_{fast}$ on the lanthanum concentration (Figure 12A) is justified. Under these circumstances, comparison of equation (16) with equation (11) shows that $k_{f,fast} = K_1'k_1$ and $k_{d,fast} = k_{-1}C_{Cu}$.

In first step of the slow phase the Cu[12-MC-4]La intermediate reacts with the ligand molecules added in excess. The kinetic behavior, shown in Figures 12B and 13B, agrees with equation 17 which have been derived as described in the SI.

$$\frac{1}{\tau_{slow}} = \frac{K_2'k_2C_{La}C_L}{(1+\dfrac{K_1}{C_{Cu}}+K_2'C_L)C_{La}+K'_1} + k_{-2} \tag{17}$$

Comparison of equation (17) with equation (12) shows that $k_{d,slow} = k_{-2}$ and, if the values of C_{Cu} and C_L are kept constant, $k_{f,slow} = K_2'k_2/(1+K_1/C_{Cu} + K_2'C_L)$.

EPR measurements. Figure 15 shows the EPR spectrum of a mixture of $CuCl_2$ and Alaha (spectrum a) and a spectrum of the same mixture in the presence of an excess of $LaCl_3$ (spectrum b). Both spectra have been recorded at pH 4.5 and I = 0.1M (NaCl). The analysis of spectrum (a) has shown that this spectrum is originated by the contributions of two mononuclear species that we denote as 4O and 2N2O. In the species 4O, copper is coordinated to four oxygen atoms, whereas in the species 2N2O copper is coordinated to two oxygen and two nitrogen atoms. Comparison of spectrum (b) with spectrum (a) shows that addition of La(III) causes the increase of the peaks associated to the 4O species.

ESI-mass spectrometry. An ESI-MS study was performed in order to verify the formation of

La[15-MC-5] when adding La(III) to the Cu(II)/Alaha solution, and in the attempt to observe the formation of reaction intermediates. The spectrum of the solution is reported in Figure 10S. the relevant detected peaks correspond to species containing the 15-MC-5 residue: $[LaCu_5L_5]Cl^{2+}$ (*m/z* 501), $[LaCu_5L_5]CH_3COO^{2+}$ (*m/z* 513), $[LaCu_5L_5]Cl_2^{+}$ (*m/z* 1037) and $[LaCu_5L_5]CH_3COOCl^{+}$ (*m/z* 1060).

Discussion

Formation of Cu^{2+}[12-MCCu(Alaha)-4]

Static experiments   The ITC titration reveals, the presence of species of stoichiometry M:L=2:1 (the dinuclear complex) and M:L=5:4 (Cu^{2+}[12-MC-4]). Also, FAB-MS analysis shows the presence of Cu^{2+}[12-MC-4]. Concerning the thermal decomposition of Cu^{2+}[12-MC-4], the negative enthalpy value of reaction (1), evaluated by DSC (Figure 2), indicates that this reaction is a combination of two processes. Actually, the heating of the solution should first induce the collapse of the ring according to reaction (1') followed by the fast protonation of the ligand according to reaction (1'')

$$Cu_5L_4^{2+} \rightleftarrows 5Cu + 4L^- \qquad\qquad (1^{'})$$

$$4L^- + 12H^+ \rightarrow 4H_3L^+ \qquad\qquad (1^{''})$$

The sudden decrease of the system absorbance at T>73°C (Figure 3B) agrees with reaction (1') and reveals that this reaction is endothermic. The protonation of the ligand, according to reaction (1'') is a strong exothermic process[9] and the combination of two processes does justify the negative value of the enthalpy of reaction (1).

Kinetic experiments. The reaction rate of the fast phase is much lower than expected for ligand substitution in the coordination shell of Cu^{2+} aquo ion.[33] This fact excludes that any of the possible steps which involve replacement of water coordinated to Cu(II) could be rate determining. Rather, it suggests that the key process in reaction (4) is the loss of a ligand molecule. The most logic

16

consequence of a reactive act between two $CuHL^+$ ions is the fast formation of a transient dimer, which looses a ligand molecule in a subsequent, rate determining step . Hence, reaction (4) can be depicted in more detailed way according to equation (18).

$$2\ CuHL^+ \overset{fast}{\rightleftarrows} Cu_2(HL)_2^{2+} \overset{slow}{\rightleftarrows} Cu_2L^{2+} +\ H_2L \qquad\qquad (18)$$

According to Pecoraro's suggestion,[4] the dinuclear complex provides the rationale for metallacrown formation and seems to constitute the basic brick in the process of formation of the Cu^{2+}[12-MC-4] metallacrown here investigated. At the best of our knowledge, the only characterized dinuclear complex of a hydroxamic acid in aqueous solution derives from the complexation of Fe(III) by salicylhydroxamic acid.[34] The formation of a dinuclear complex as a precursor of Cu^{2+}[12-MC-4] formation is here confirmed by ITC experiments. It should also be noted that single point energy calculations, that we have performed by using the HyperChem software, have also shown that the transition from the dimer to the dinuclear complex (second step of process (18)) is energetically favoured (ΔE = -6.3 kcal mol^{-1}).

On the other hand, dimeric structures were proposed by Paniago and Carvalho[19] and Farkas and coworkers,[23]. While the former authors suggest the structure D1, the latter suggest the structure D2 (Scheme 1). However, a more recent investigation by Tegoni and coworkers[16] does not provide any evidence for the presence of the dimeric species in solution under the condition of metal excess. This finding agrees with the present results which suggest, for $C_{Cu} \gg C_L$, the dinuclear complex is formed (reaction (7)) as the MC precursor instead of the dimer. In this work, however, dimer formation is reconsidered as a transient precursor in reaction (4) which is operative when C_{Cu} is similar to C_L. In fact, indirect evidence for dimer could be suggested by the presence of a tetramer revealed by FAB-MS analysis. Of the two structures shown in Scheme 1, the structure D2, which corresponds to the repetitive unit of Cu^{2+}[12-MCCu(Alaha)-4], should be considered as the correct one.

D1   **D2**   **D3**
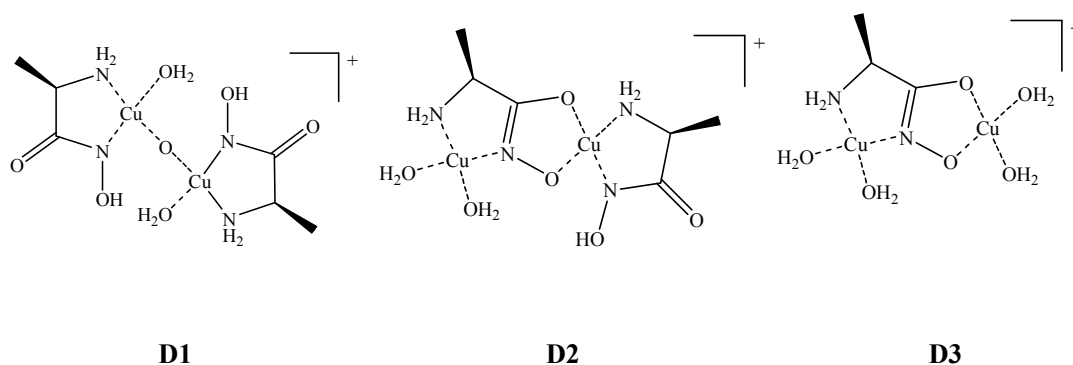
Scheme 1. *Possible structures for the Cu(II)/Alaha dimer (D1, D2) and proposed structure for the dinuclear complex.*

Concerning the kinetics of the slow phase, the formation of Cu^{2+}[12-MC-4] is clearly revealed by the slower of the two effects displayed by the kinetic curve of Figure 5. Actually the amplitude of this effect changes with pH according to the trend shown in Figure 8. The range of existence of the metallacrown (3.5 < pH < 6.0) is the same as that observed by Tegoni et al.[20] by pH-metric titration. Likely, the slow phase corresponds to an evolution of the Cu_2L^{2+} species with successive addition of Cu^{2+} and L^{2-} components, which stops when the cyclic structure of Cu_5L_4 has been completed. We put forward the hypothesis that Cu_2L^{2+} first goes through dimerization with formation of a tetranuclear $[Cu_4L_2]^{4+}$ complex, and then that the latter species evolves into the assembled metallacrown. This hypothesis is in agreement with that proposed recently by Pecoraro and coworkers,[35] which also isolated the tetranuclear species in the solid state. Therefore, the formation of the Cu_2L^{2+} species is the process which actually initiates the assembly of the 12-MC-4 complex. The phase of formation of the dinuclear complex corresponds therefore to the nucleation process, while the second phase could be seen as the growth of the nucleus. The slow process could be composed of consecutive and coordinated steps, with similar reaction rates and with the same proton dependence. It should finally be noted that experiments performed at $C_L > C_{Cu}$ display only the fast kinetic effect, suggesting that under these circumstances the reactive process stops at the

18

level of reaction (4), thus confirming that Cu^{2+}[12-MC-4] does not form in the absence of copper excess.

Reaction between Cu^{2+}[12-MCCu(Alaha)-4] and Lanthanium(III)

When this work was in progress a paper appeared describing the kinetics of the Ca^{2+} ion replacement by Ln^{3+} in Ca(II)[15-MC$_{Cu(II)(Trpha)}$-15].[8] Whereas in that system the replacement process is described in terms of a single-step reaction, the results concerning the system here investigated show that the metal substitution process does occur in two phases. The data shown in Figure 13 reveal, surprisingly but unequivocally, that the Cu^{2+} ion is expelled from the core of Cu^{2+}[12-MC-4] as a consequence of the interaction of the metallacrown with La^{3+} in the fast phase of the process. This phase involves the intermediacy of the ternary intermediate Cu[12-MC-4]La (reaction 14) and ends with the formation of the La[12-MC-4] complex, where lanthanum(III) is likely coordinated side-on to the 12-MC-4 cavity as found for the lanthanide adduct with the zinc(II)-picolinehydroxamate metallacrowns.[36] The formation of the bimetallic Cu[12-MC-4]La is fundamental to explain the observed kinetic behavior and, on the other hand, indicates the associative character of the fast phase. Note that a similar associative mode of activation has been proposed for the reaction of Ca(II) replacement by La(III) in Ca(II)[15-MC$_{Cu(II)(Trpha)}$-15].[8] The fast phase does not need the presence of excess ligand, as shown by the behaviour displayed in Figure 14A which reveals that the fast kinetic effect is independent of the ligand concentration. On the contrary, the dependence of the rate of the slow phase is dependent on the ligand concentration, thus supporting the hypothesis that Cu[12-MC-4]La is the relevant species which participates to the process leading to La[15-MC-5]. Attempts to detect the intermediates of the slow phase reaction by ESI-MS resulted unsuccessful, as the observed peaks all refer to the final La[15-MC-5] species. However, although unstable, a bimetallic Cu[12-MC-4]La may likely contain the Cu^{2+} and the La^{3+} cations as coordinated side-on to the cavity of the 12-MC-4 on two different faces, in analogy with that observed recently in heterometallic 12-MC-4 complexes.[37]

The slow phase is therefore completed in two steps. In the first step a molecule of Alaha from the solution binds to copper in the Cu[12-MC-4]La complex to give the species CuL[12-MC-4]La. The driving force for this step is provided by the strong affinity of Cu(II) for Alaha , also considered the presence of an unsaturated coordination shell on Cu^{2+} as the result of its partial displacement from the cavity. Owing to its extreme kinetic lability,[33] the partially displaced Cu^{2+} ion can bind very rapidly a molecule of Alaha therefore accounting for a very fast formation of the CuL[12-MC-4]La intermediate. Note that, in this species, the copper atom bound side-on in principle could bind the acetate ions present in solution. If this is the case, the species with one AcO^- ions bound to the metallacrown, detected in the ESI experiments, could be associated with the above intermediate. The second (rate determining) step of the slow phase results in the formation of the La[15-MC-5] product, likely obtained by the insertion of the CuL fragment into the 12-MC-4 scaffold with formation of the 15-MC-5 framework. This step involves bond breaking and bond reforming in the crown, hence it requires a relatively high energy penalty, which reflects in a reduced rate of reaction.

The EPR experiments corroborate the conclusions derived from the kinetic study. Actually Figure 15 shows that addition of La(III) causes the increase of the peaks associated to the 4O monomer (signal A) and, at the same time, the decrease of the peaks associated to the monomer 2N2O (signal B). This means that, as $LaCl_3$ and monomer 2N2O are added to the solution containing the Cu^{2+}[12-MC-4] metallacrown. At the same time, a mononuclear species is formed where the copper ion is coordinated by four oxygen atoms. This observation agrees with step 14 where the central Cu(II) ion is expelled and is immediately coordinated by oxygen atoms coming from the acetate buffer or/and water molecules.

Acknowledgements

Table 1 Apparent kinetic parameters for the $Cu^{2+}[12\text{-MCCu(Alaha)-4}]$/La(III) reaction. I = 0.1 M, pH = 4.5, T = 25°C.

10 $k_{f,fast}$	$10^3 k_{d,fast}$	K_{fast}	$10^4 k_{f,slow}$	$10^4 k_{d,slow}$	K_{slow}
$(M^{-1}s^{-1})$	(s^{-1})	(M^{-1})	(s^{-1})	(s^{-1})	
1.9±0.1	5.6±0.2	33.2±0.3	5.5±0.1	1.4±0.1	4.0±0.2
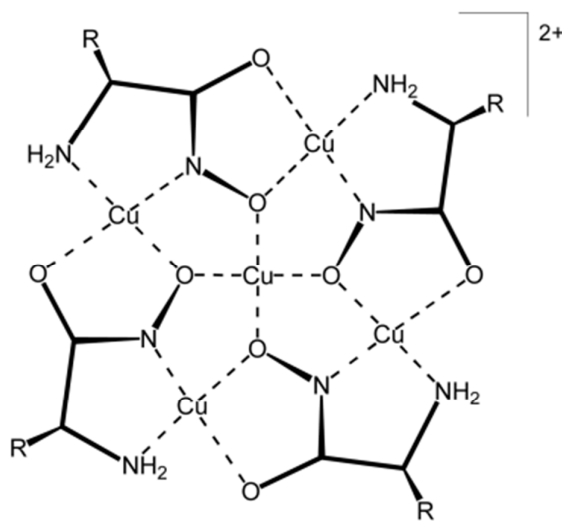
Figure 1. *Representation of the 12-MC-4 metallamacrocycle of Cu(II) and (S)-α-aminohydroxamic acid (Alaha). Note that both the OH and NH sites loose their protons upon Cu(II) complexation.*
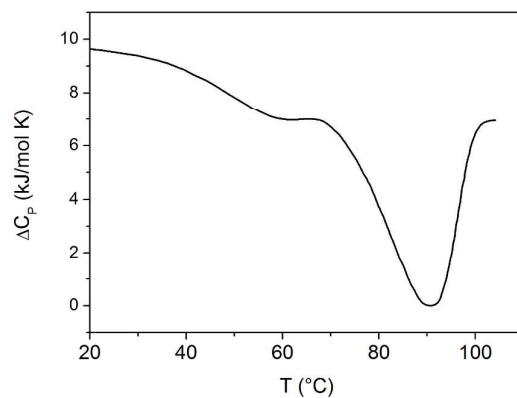
Figure 2. *DSC curve for the Cu(II)/Alaha system; $C_{CuCl2}= 1.0 \times 10^{-2}$ M, $C_{Alaha}= 8.0 \times 10^{-3}$ M, $I = 0.1$ M (KCl), scan rate $= 1°C/min; P = 1.5$ atm; pH = 4.5.*
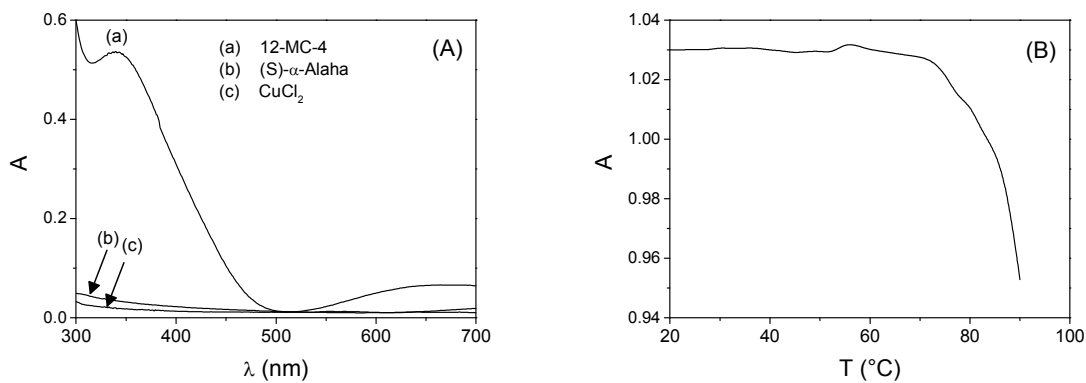
Figure 3. (A) *Absorbance spectra for the Cu(II)/Alaha system; $C_{CuCl2}= 1.2 \times 10^{-3}$ M, $C_{Alaha}= 1.5 \times 10^{-3}$ M, $C_{Cu2+[12-MCCu(Alaha)-4]} = 1.33 \times 10^{-4}$ M, pH = 4.5, I = 0.1 M and T = 25 °C.* (B) *Absorbance dependence on temperature for the Cu(II)/Alaha system; pH = 4.75, I = 0.1 M and λ = 340 nm.*
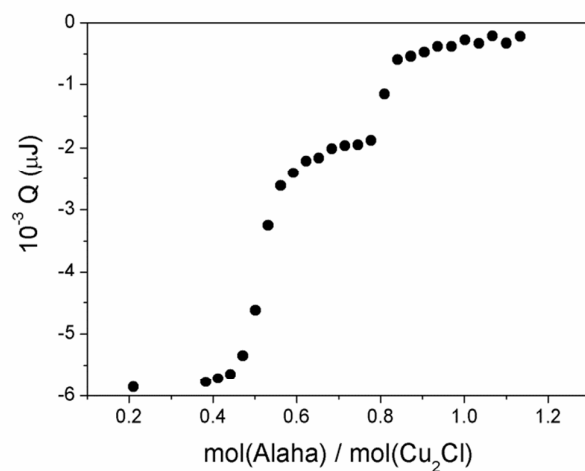
Figure 4. *ITC curve for the Cu(II)/Alaha system. pH = 4.5, I = 0.1 M and T = 25 °C. C_{CuCl2}=*

3.2×10^{-2} M.
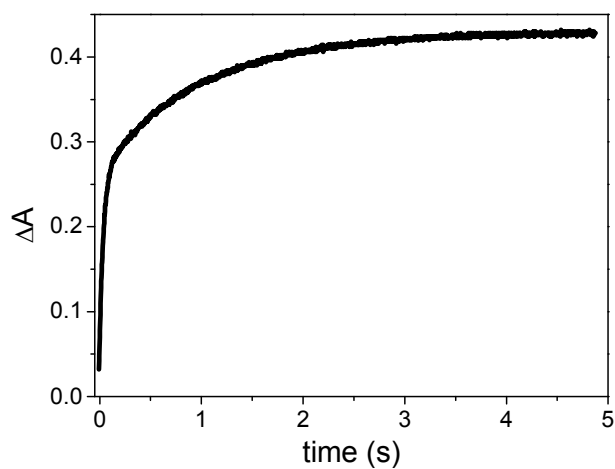
Figure 5. *Stopped-flow trace recorded for the Cu(II)/Alaha system; C_{CuCl2} = 1.0×10^{-2} M, C_{Alaha}=*

4×10^{-4} M, pH = 4.5, I = 0.1 M, λ = 340 nm, T = 25 °C.
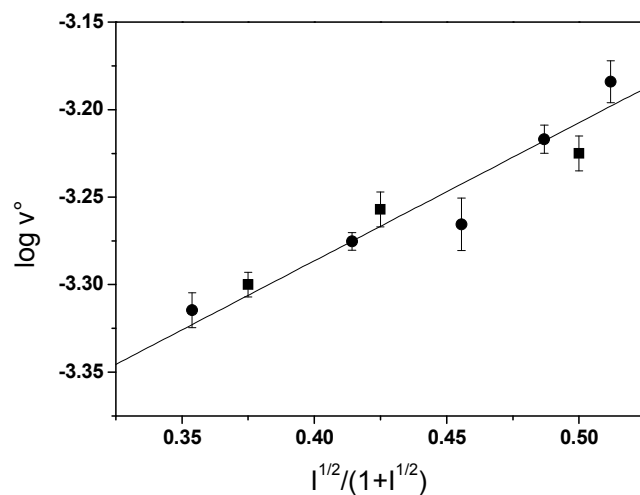
Figure 6. *Dependence of the logarithm of the initial rate on ionic strength, according to equation (2), for the Cu(II)/Alaha system; $C_{CuCl2} = 6.25\times10^{-4}$ M, $C_{Alaha} = 5.0\times10^{-4}$ M, pH = 4.5, T = 25 °C, ●KCl, ■NaClO$_4$.*
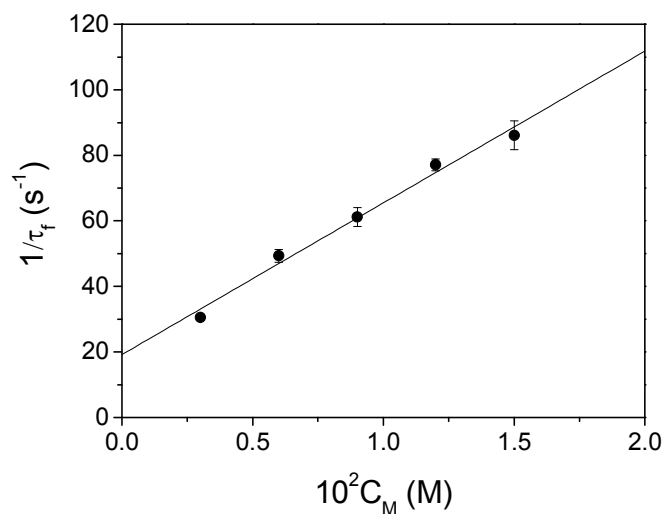
Figure 7. *Dependence of the reciprocal fast relaxation time for the Cu(II)/Alaha system on the metal concentration under metal excess conditions ($C_M >> C_L$); $C_L = 3.0\times10^{-4}$, I = 0.1 M, pH = 4.5, T = 25 °C. Straight line drawn according to equation (8).*

25
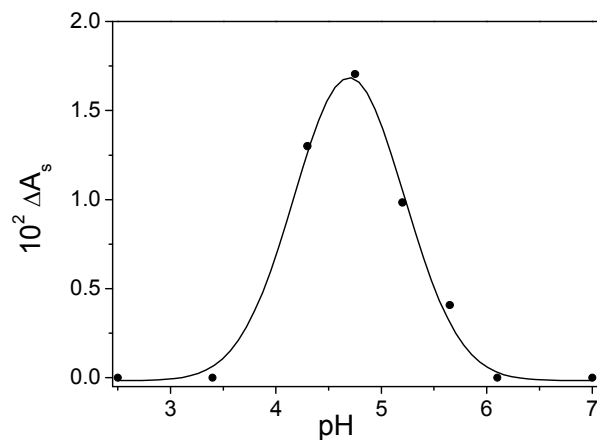
Figure 8. *pH dependence of the amplitude for slow kinetic effect for the Cu(II)/Alaha system;* $C_{CuCl2} = 6.25 \times 10^{-4} M$, $C_{Alaha} = 5.0 \times 10^{-4} M$, *pH=4.5, I = 0.1 M, λ = 340 nm and T = 25 °C.*
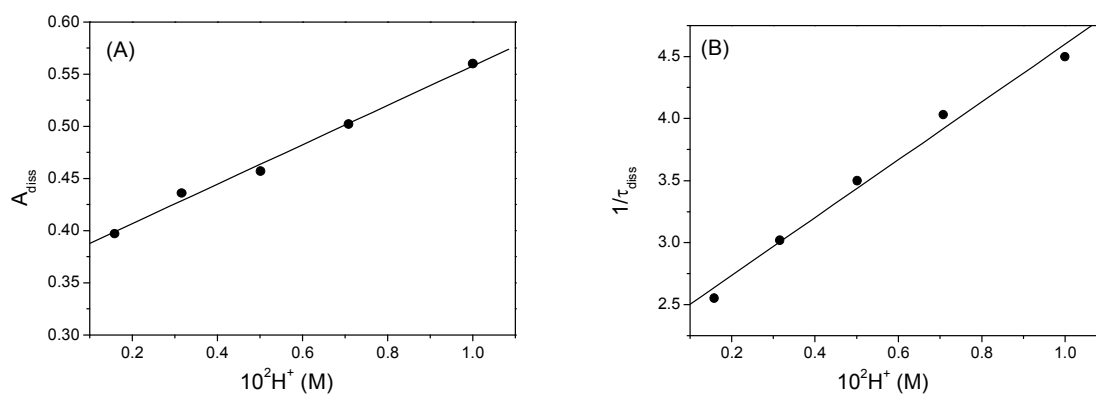
Figure 9. *Dependence of amplitudes (A) and time constants (B) on [H^+] for the reaction of* Cu^{2+} *[12-MC-4] dissociation; I = 0.1 M, λ = 340 nm, T = 25 °C.*
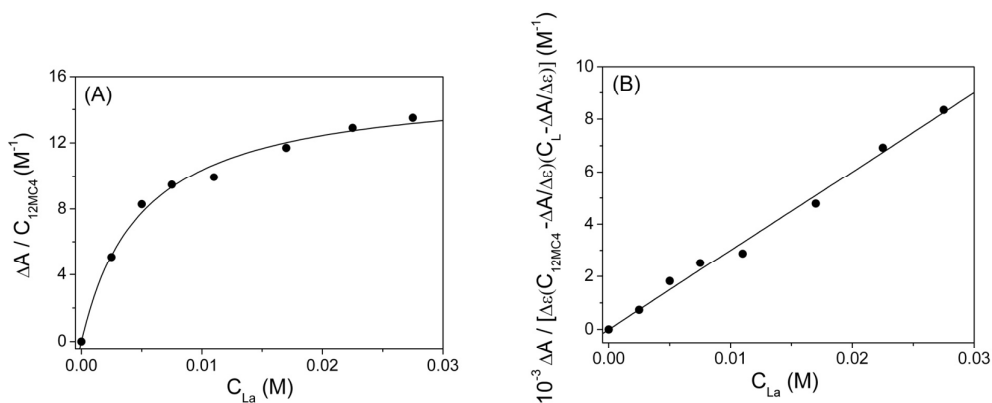
Figure 10. Binding isotherm (A) and data analysis according to equation (9) (B) for the reaction between Cu^{2+}[12-MC-4] and La(III); C$_{Cu[12-MC-4]}$=5.0×10^{-4}M, C$_L$ =5.0×10^{-4}M, I = 0.1 M, pH = 4.5, λ= 580 nm, T = 25°C.
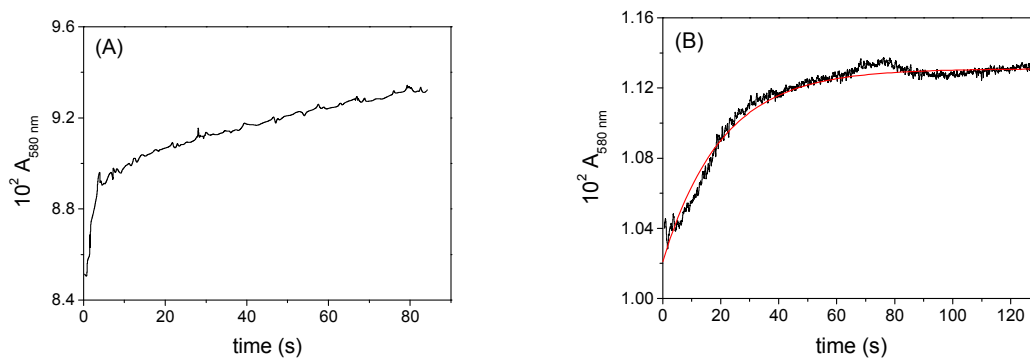
Figure 11. (A) Biphasic kinetic curve for the reaction of Cu^{2+}[12-MC-4] with La(III); C$_{La}$ = 3.9×10^{-2} M; C$_{Cu}$ = 3×10^{-3} M, C C$_{Alaha}$ = 3×10^{-3} M, I = 0.1 M, pH = 4.75, λ = 580nm, T = 25°C. (B) Monophasic kinetic curve for the reaction of Cu^{2+}[12-MC-4] with La(III) and excess Cu(II); C$_{La}$ =1.23×10^{-1} M, C$_{Cu}$ = 1×10^{-2} M, C$_{Alaha}$ = 3×10^{-3} M pH = 4.5, λ = 580nm, T = 25°C.

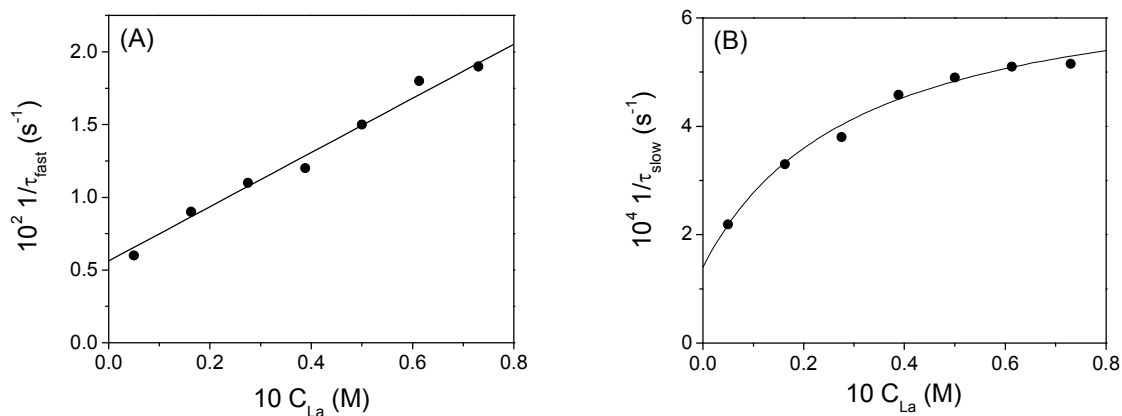*Figure 12. Dependence of the time constants on La(III) concentration for the fast (A) and slow(B) kinetic effect observed for the Cu²⁺[12-MC-4] /La(III) reaction. I = 0.1 M, pH = 4.5, T = 25°C.*
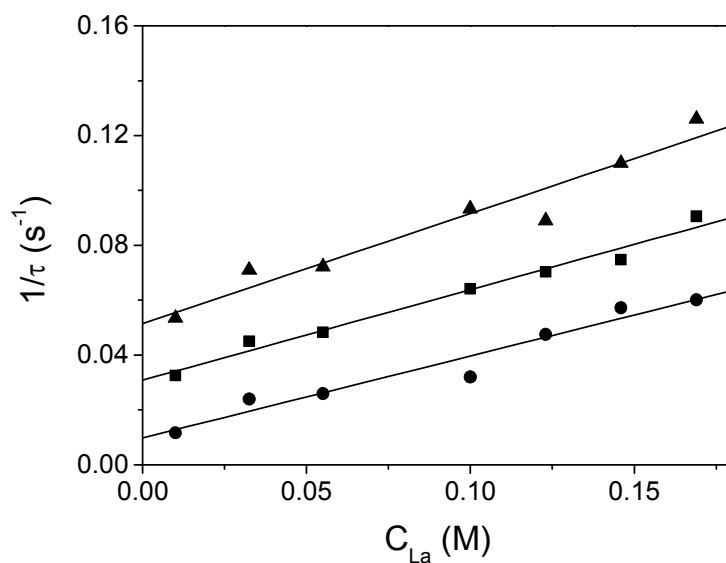

Figure 13. Rate constants dependence on La(III) concentration for the fast kinetic effect observed for the Cu²⁺[12-MC)-4]/La(III) reaction with different excess Cu(II) concentrations. ● C_Cu = 1×10⁻² M; ■ C_Cu = 2.5×10⁻² M, ▲ C_Cu = 5×10⁻² M, pH = 4.5, I = 0.1 M, T = 25°C.
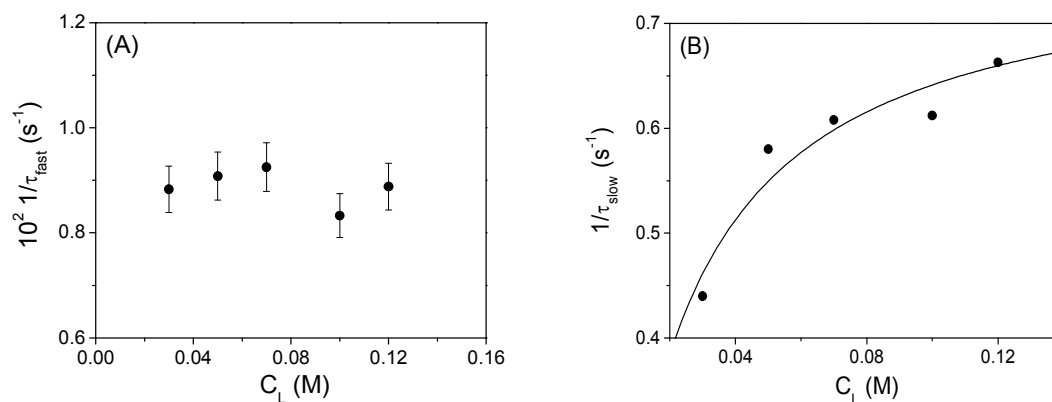
Figure 14. *Time constant dependence on the Alaha concentration(C_L) for the fast (A) and slow (B) kinetic effects observed for the Cu^{2+}[12-MC-4]/La(III) reaction. pH = 4.5, I = 0.1 M, T = 25°C.*
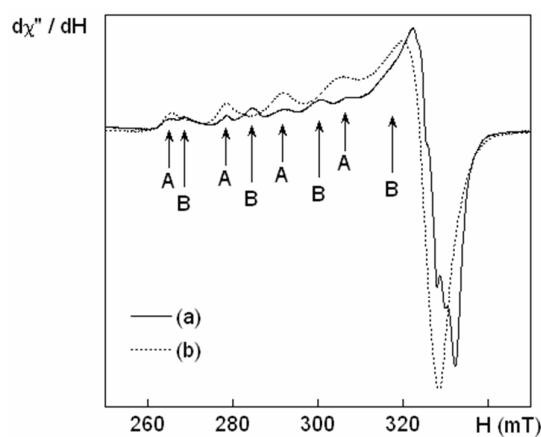

Figure 15. *Comparison of the EPR spectra of solutions containing Cu(II) ions and Alaha in acetate buffer (pH=4.5) before (a) and after (b) the addition of La(III) ions. T=150 K, modulation amplitude 5 G, time constant 40.96 ms, conversion time 327.68 ms, gain 6.32 10^4, power 20 mW, microwave frequency 9.4201 (a) and 9.4182 (b) GHz.*

REFERENCES

1   *V. L. Pecoraro, A. J. Stemmler, B. R. Gibney, J. J. Bodwin, H. Wang, J. W. Kampf and A. Barwinski, Prog. Inorg. Chem., 1997, **45**, 83.*

2   *J. J. Bodwin, A. D. Cutland, R. G. Malkani and V. L. Pecoraro, Coord. Chem. Rev., 2001, **216**, 489.*

3   *M. Tegoni and M. Remelli, Coord. Chem. Rev., 2012, **256**, 289.*

4   *G. Mezei, C. M. Zaleski and V. L. Pecoraro, Chem. Rev., 2007, **107**, 4933.*

5   *C. Lim, A. C. Van Noord, J. W. Kampf and V. L. Pecoraro, Abstr. Pap. Am. Chem. Soc., 2007, **233**, 906.*

6   *M. S. Lah and V. L. Pecoraro, J. Am. Chem. Soc., 1989, **111**, 7258.*

7   *V. L. Pecoraro, Inorg. Chim. Acta, 1989, **155**, 171.*

8   *C. S. Lim, M. Tegoni, T. Jakusch, J. W. Kampf and V. L. Pecoraro, Inorg. Chem., 2012, **51**, 11533.*

9   *C. S. Lim, J. W. Kampf and V. L. Pecoraro, Inorg. Chem., 2009, **48**, 5224.*

10 *M. Tegoni, M. Tropiano and L. Marchio, Dalton Trans., 2009, 6705.*

11 *M. Tegoni, M. Furlotti, M. Tropiano, C. S. Lim and V. L. Pecoraro, Inorg. Chem., 2010, **49**, 5190.*

12 *B. R. Gibney, D. P. Kessissoglou, J. W. Kampf and V. L. Pecoraro, Inorg. Chem., 1994, **33**, 4840.*

13 *M. Tegoni, M. Remelli, D. Bacco, L. Marchio and F. Dallavalle, Dalton Trans., 2008, 2693.*

14 *T. N. Parac-Vogt, A. Pacco, P. Nockemann, Y. F. Yuan, C. Gorller-Walrand and K. Binnemans, Eur. J. Inorg. Chem., 2006, 1466.*

15 *S. H. Seda, J. Janczak and J. Lisowski, Inorg. Chim. Acta, 2006, **359**, 1055.*

16 *F. Dallavalle, M. Remelli, F. Sansone, D. Bacco and M. Tegoni, Inorg. Chem., 2010, **49**, 1761.*

17 *A. J. Stemmler, J. W. Kampf, M. L. Kirk, B. H. Atasi and V. L. Pecoraro, Inorg. Chem., 1999, **38**, 2807.*

18 *M. Tegoni, L. Ferretti, F. Sansone, M. Remelli, V. Bertolasi and F. Dallavalle, Chem. - Eur. J., 2007, **13**, 1300.*

19 *H. Diebler, F. Secco and M. Venturini, J. Phys. Chem., 1984, **88**, 4229.*

20 *M. Careri, F. Dallavalle, M. Tegoni and I. Zagnoni, J. Inorg. Biochem., 2003, **93**, 174.*

21 *E. Lange and A. L. Robinson, Chem. Rev., 1931, **9**, 89.*

22 *D. Marquardt, J. Soc. Ind. Appl. Math., 1963, **11**, 431.*

23 *E. Farkas, J. Szoke, T. Kiss, H. Kozlowski and W. Bal, J. Chem. Soc. Dalton. Trans., 1989, 2247.*

24 *E. B. Paniago and S. Carvalho, Inorg. Chim. A. - Bioinor., 1984, **92**, 253.*

25 *J. H. Van't Hoff and E. Cohen, (Ed.: E. Muller), 1896, p. 286.*

26 *A. A. Frost and R. G. Pearson, Kinetics and mechanisms, John Wiley & Sons, New York London, 1961.*

27 *J. E. Prue, Pergamon Press, 1966, p. 115.*

28 *E. Guntelberg, Z. Phys. Chem., 1926, **123**, 199.*

29 *T. Biver, F. Secco, M. R. Tine and M. Venturini, J. Inorg. Biochem., 2004, **98**, 33.*

30 *B. Garcia, J. M. Leal, R. Ruiz, T. Biver, F. Secco and M. Venturini, J Phys Chem B, 2010, **114**, 8555.*

31 *T. Biver, F. Secco and M. Venturini, Arch Biochem Biophys, 2005, **437**, 215.*

32 *T. Biver, M. Pulzonetti, F. Secco, M. Venturini and S. Yarmoluk, Arch Biochem Biophys, 2006, **451**, 103.*

33   *J. Burgess, Metal ions in solution, Ellis Horwood Limited, Chichester, 1978.*

34   *M. R. Beccia, T. Biver, B. Garcia, J. M. Leal, F. Secco and M. Venturini, Inorg. Chem., 2011, **50**, 10152.*

35   *J. Jankolovits, J. W. Kampf and V. L. Pecoraro, Inorg. Chem., 2013, **52**, 5063–5076.*

36   *J. Jankolovits, C. M. Andolina, J. W. Kampf, K. N. Raymond and V. L. Pecoraro, Angew Chem Int Edit, 2011, **50**, 9660.*

37   *M. R. Azar, T. T. Boron, J. C. Lutter, C. I. Daly, K. A. Zegalia, R. Nimthong, G. M. Ferrence, M. Zeller, J. W. Kampf, V. L. Pecoraro and C. M. Zaleski, Inorg. Chem., 2014, **53**, 1729.*

Graphical and textual abstract
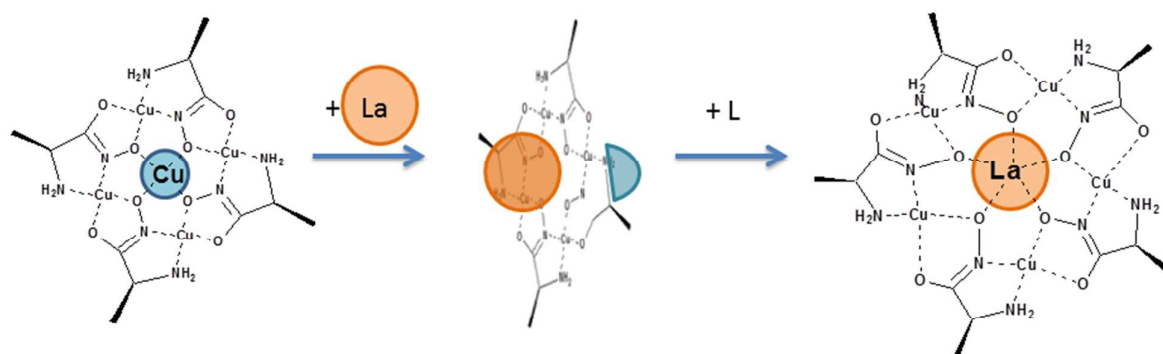
A kinetic and thermodynamic study of the formation of Cu^{2+}[12-MC-4] metallacrown from Cu(II) and α-alaninehydroxamic acid shows that the dinuclear complex Cu_2L^{2+} plays a fundamental role in the crown assembly. La^{3+} promotes the enlargement of the Cu^{2+}[12-MC-4] crown and is in turn encapsulated in the central cavity as La^{3+}[15-MC-5]. The key intermediate of the process is the Cu[12-MC-4]La ternary complex.